

# Effect of Finite Granularity of Detector on Anisotropy Coefficients

Rashmi Raniwala<sup>1</sup>, Sudhir Raniwala<sup>1</sup>, Yogendra Pathak Viyogi<sup>2</sup>

<sup>1</sup> Physics Department, University of Rajasthan, Jaipur 302004, India

<sup>2</sup> Variable Energy Cyclotron Centre, Calcutta 700064, India

e-mail: *raniwala\_jp1@sancharnet.in*

## 1 Introduction

Over the last one decade, elliptic flow in ultrarelativistic heavy ion collisions has become an important probe of the dynamics of the system [1]. The elliptic flow manifests itself as an anisotropy in the azimuthal distributions of transverse momentum of the emitted particles. The azimuthal distributions are expanded in a Fourier series where the coefficients of expansion are the measures of different orders of anisotropy [2]. Large number of experiments have measured the elliptic flow of different particle species in different kinematic domains for a variety of colliding systems and a range of center of mass energies [3, 4, 5, 6, 7, 8, 9]. These measurements have provided new perspectives attempting to explain the observed mass dependence of the elliptic flow [10].

In experiments where  $p_T$  is not measured, the anisotropy coefficients are determined from the azimuthal distribution of the number of particles. Detectors in some experiments measure the distribution of hits<sup>1</sup>. Anisotropy coefficients describing distribution of hits is expected to be smaller than coefficients describing distribution of particles;  $v_n^{hits} < v_n$  and there is need to determine an appropriate correction factor to obtain  $v_n$  from the measured values of  $v_n^{hits}$ . In the present work, we obtain an approximate expression for the ratio  $\frac{v_n^{hits}}{v_n}$ , and corroborate the results with simulation results.

## 2 Multiple Hits and Azimuthal Anisotropy

An actual experiment, as against a simulation experiment, has a finite number of detector cells  $N_{cells}$ , which defines the coarseness of the granularity for a given acceptance of the detector. For a given number of incident particles,  $N_{part}$ , one can define the mean occupancy  $\mu_0$

$$\mu_0 = \frac{N_{part}}{N_{cell}} \quad (1)$$

The probability of  $n$  particles incident on any cell is

$$P_n = \frac{\mu_0^n \cdot e^{-\mu_0}}{n!} \quad (2)$$

This gives

$$\frac{N_{hit}}{N_{part}} = \frac{1 - e^{-\mu_0}}{\mu_0} = \frac{-x}{\ln(1 - x)} \quad (3)$$

where  $x = N_{hit}/N_{cell}$  is experimentally measurable. Mean occupancy can also be written as  $\mu_0 = -\ln(1 - x)$ . Writing the total number of cells as the sum of occupied and unoccupied cells, one can immediately obtain the expression for occupancy as in ref [9].

$$\mu_0 = \ln\left(1 + \frac{N_{occ}}{N_{unocc}}\right) \quad (4)$$

<sup>1</sup>One activated cell is counted as  $N_{hit} = 1$  irrespective of the number of tracks activating it.

enabling its determination from experimentally measurable quantities.

Since the intrinsic occupancy of cells increases with the increase in the number of incident particles, the occupancy will have the same azimuthal dependence as the incident particles. Using this for the occupancy in equation 3 gives the azimuthal dependence of the hits as

$$N_{hits} \propto 1 - e^{-(1+\sum 2v_n \cos n(\phi - \psi_n))} \quad (5)$$

Expressing the resulting equation as a Fourier series and collecting coefficients of  $\cos n(\phi - \psi_n)$  enables a determination of the ratio  $v_n^{hits}/v_n$ , which to first order can be approximated as

$$\frac{v_n^{hits}}{v_n} = \frac{1 - \mu_0 + \frac{\mu_0^2}{2} - f(v)}{1 - \frac{\mu_0}{2} + \frac{\mu_0^2}{6}} \quad (6)$$

Function  $f(v)$  contributes when both occupancy and flow are large and is

1.  $f(v) = \mu_0 v_2$  for  $n = 1$ .
2.  $f(v) = \frac{\mu_0 v_1^2}{2v_2}$  for  $n = 2$ .

The ratio can also be approximated as

$$\frac{v_n^{hits}}{v_n} = -\frac{1-x}{x} \cdot \ln(1-x) \quad (7)$$

These results have been corroborated with results from simulations as described in the following.

### 3 Simulation and Analysis

Simulation experiments involve two steps: event generation and analysis. For the purpose of the present work, one needs to know the azimuthal distribution of the hits and of the particles for each event, since the analysis is based only on these variables. Detector geometry, flow and occupancy are varied for a systematic study.

Multiplicities for the events are generated so that these are commensurate with the range of occupancies in various experiments. Assuming a constant  $dN/d\eta$  and an exponential  $p_T$  distribution, the kinematic variables of each particle are generated with  $p_T$  in the region 0 to 6 GeV/c and  $\eta$  in the region of acceptance of the detector. Azimuthal angles of each particle is assigned according to

$$r(\phi) = \frac{1}{2\pi} [1 + 2v_1 \cos(\phi - \psi_R) + 2v_2 \cos 2(\phi - \psi_R)] \quad (8)$$

Events are simulated for different granularities in  $\eta$  and  $\phi$ . A constant  $dN/d\eta$  distribution and cells of equal  $\delta\eta$  intervals give a uniform intrinsic occupation probability for each cell.

For the present work, we assumed  $\Delta\eta$  acceptance of detector equal to 0.56 and divided this region into 8, 40 and 64 equal intervals. The acceptance and the divisions are fairly arbitrary but commensurate with the coarseness of certain detectors [11, 12]. More specifically, simulations were performed for

- $\Delta\eta = 0.07$ ,  $\Delta\phi = 2^\circ$  (1440 channels)
- $\Delta\eta = 0.014$ ,  $\Delta\phi = 10^\circ$  (1440 channels)

- $\Delta\eta = 0.00875$ ,  $\Delta\phi = 10^\circ$  (2304 channels)

The results are based on an analysis of  $10^6$  events. For low flow values, the number of generated events is  $2.5 \cdot 10^6$ .

The number of particles simulated and number of cells activated ( $N_{hits}$ ) are known for each event. We assume that one incident particle does not activate more than one cell(channel).

The following data sets are stored from the simulated data.

1. azimuthal angles of all particles (infinite granularity detector).
2. azimuthal angles of the cells for all incident particles (finite azimuthal size of each cell and signal proportional to number of particles entering the cell).
3. azimuthal angles of all hits (finite azimuthal size of each cell and binary (hit/no-hit) signal from each cell).

The simulated data is analysed for all detector geometries described above.

$n^{th}$  order Fourier coefficients can be determined from the azimuthal distribution of the particles with respect to the event plane angle of order  $m$ , provided  $n$  is an integral multiple of  $m$ , by fitting to the following equations [2]

$$\frac{dN}{d(\phi - \psi'_m)} \propto 1 + \sum_{n=1}^{\infty} 2v'_{nm} \cos nm(\phi - \psi'_m) \quad (9)$$

The event plane angle and its resolution are obtained by methods described in [2].

In the present work, Fourier coefficients  $v'_{nm}$  are extracted for the case with event plane order equal to the order of the extracted Fourier coefficient, i.e.  $v'_{nm} = v'_{nn}$  and is denoted here by  $v'_n$ . Different methods are used. Each event is divided into two subevents based on geometry while preserving the gross azimuthal symmetry.

1.  $v'_n^a = \langle \cos n(\phi^a - \psi'_n^b) \rangle$  and  $v'_n^b = \langle \cos n(\phi^b - \psi'_n^a) \rangle$  are determined where  $\phi^a$  represent the azimuthal angles of particles in subevent  $a$  and  $\psi'_n^b$  is the event plane angle determined using particles in subevent  $b$ . The averages are computed over all particles over all events. In the absence of non flow correlations [13]

$$v_n = \sqrt{\frac{v'_n^a \cdot v'_n^b}{\langle \cos n(\psi'_n^a - \psi'_n^b) \rangle}} \quad (10)$$

2. Extract  $v'_n$  by fitting equation 9 to the  $\phi - \psi_n$  distribution obtained by filling particles of one subevent with respect to the other subevent plane angle. This yields

$$v_n = \frac{\sqrt{2} \cdot v'_n}{RCF_n} \quad (11)$$

The factor  $\sqrt{2}$  occurs because the event plane is determined using half of the event multiplicity.

3.  $v_n$  is also obtained directly by subevent method from  $\chi_n$  using [14]

$$v_n = \frac{\chi_n}{\sqrt{2M}} \quad (12)$$

The three methods listed above are equivalent, and yield same results.

4. Anisotropy coefficients are also obtained by another method. Here the  $v'_n$  values are extracted by fitting equation 9 to the  $\phi - \psi_n$  where  $\psi_n$  is obtained by excluding the particle being entered in the distribution <sup>2</sup>. The  $v_n$  values are obtained by dividing these  $v'_n$  values by  $RCF_n$  which is obtained by dividing each event randomly into two subevents of equal multiplicity. For a detector that measures the distribution of hits, this method yields results which are different from the results of the three methods mentioned above.

## 4 Results and Discussion

Simulation results on  $N_{hits}/N_{part}$  as a function of  $x$  are shown in Fig. 1 for different values of initial flow. Results obtained using equation 3 are shown as a solid line, and are seen to agree with the results of simulation.

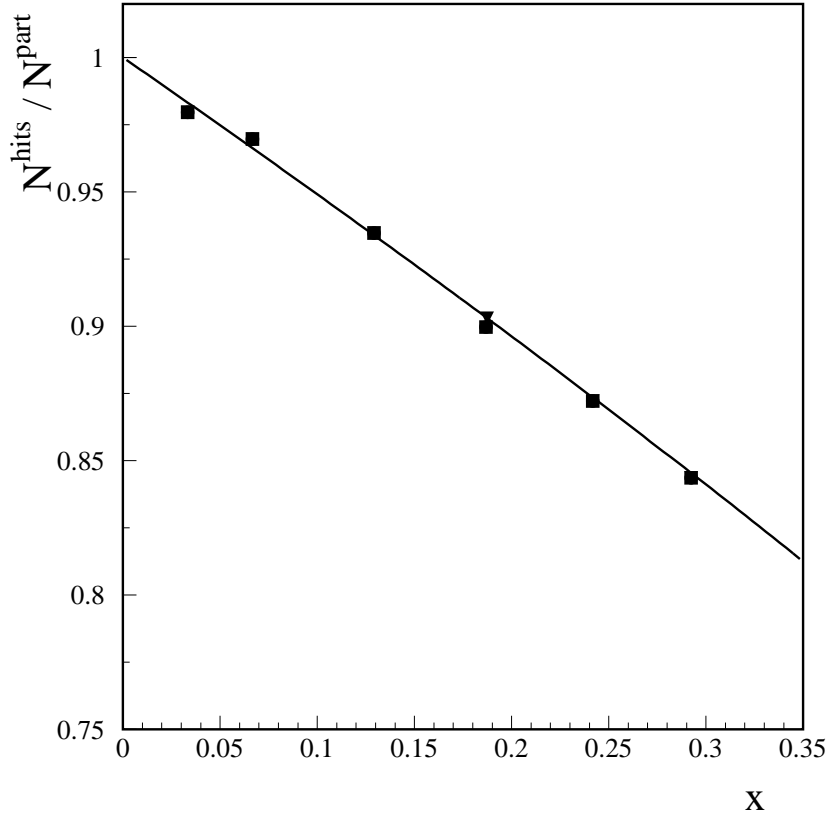


Figure 1: The ratio  $N_{hit}/N_{part}$  for different values of  $x$ . The points are from simulation and the curve is equation 3.

### 4.1 Reconstructing Anisotropy Values: Methods 1-3

The dilution in the anisotropy coefficients due to finite granularity can be computed easily using the known event plane angle in simulation. We compute  $v_n = \langle \cos(n(\phi' - \psi_{known})) \rangle$  for the different situations listed in details of data sample and obtain

---

<sup>2</sup>This avoids autocorrelations but also introduces a negative correlation, effectively decreasing the values of  $v'_n$ .

1.  $v_n^{ideal}$  using all particles and their angles. This corresponds to measurements using a detector with infinite granularity.
2.  $v_n^{ch}$  using all particles but their angles are replaced by the angles corresponding to the mean positions of the detector cells. This is equivalent to randomly adding (or subtracting)  $\Delta\Phi$  ( $\leq \frac{\Phi}{2}$ ) to each  $\phi$  where  $\Phi$  is the azimuthal size of each cell.
3.  $v_n^{hits}$  using all hits and the angles corresponding to the mean positions of the detector cells.

$v_n^{ideal}$  reproduces the input flow, as should be naively expected. The dilution due to coarse information about the particle angle can be judged by plotting the ratio  $v_n^{ch}/v_n^{ideal}$ . This has been plotted in Fig. 2 for two different values of initial anisotropy, and one does not see any deviation of this ratio from unity for the whole range of occupancy considered. This is expected for the case where the azimuthal extent of each cell is  $2^\circ$ . One does not see any significant deviation from one for an azimuthal size of  $10^\circ$ . For an azimuthal size of  $\Phi^\circ$ , the required correction factor for order  $n$  is  $\frac{\sin n\Phi/2}{n\Phi/2}$ . This has also been corroborated using simulations.

$v_n^{hits}$  will be diluted both due to coarse information of particle angle and loss of particles because of multiple hits. The results above show that the coarse information of particle angle has very little effect, and the dilution in  $v_n^{hits}$  is primarily due to multiple hits. This is best seen by plotting the ratio  $v_n^{hits}/v_n^{ideal}$  for increasing occupancies. for the simulated data. The results here are shown for a  $\Phi = 2^\circ$ . There is a small  $v$  dependence also. The solid line and the dotted line represent equations 6 and 7 respectively, and are seen to corroborate simulation results.

We wish to investigate if these results are reproduced when event plane angle is determined from data, instead of using the known angle in simulation.

Fig. 3 shows the results when the event plane angle is determined from the angles of all the particles or hits, for the three kinds of date sets. Equations 6 and 7 are shown as solid and dotted line respectively. The dashed line is equation 6 without the term  $f(v)$ . One observes that simulation results and the corrections factors obtained above corroborate each other. We can see from this that the correction factor for a detector with 30% mean occupancy increases the measured value of anisotropy ( $v_n^{hits}$ ) by about 20% to obtain the actual value of anisotropy ( $v_n$ ), clearly a significant effect.

## 4.2 Random Subdivision of Events; Method 4

In this method, loss due to multihits coupled with limitation of method for removing auto correlations and random subdivision of events results into lower values of  $v_n$ . The effect is most prominent for low values of anisotropy and multiplicity. The correction factors obtained for the finite granularity using this method are much higher and arise due to the combined effect of finite granularity and the limitation of the method of analysis. The method also limits the apparent sensitivity of detecting anisotropy in the data.

These limitations are investigated systematically and are shown in figure 4. The three panels show the uncorrected values  $v'_n$ , the event plane resolution correction factor RCF, and the resolution corected values  $v_n$  respectively. The values obtained using the distribution of particles are shown by open circles and those obtained using the distribution of hits are shown by filled circles. These values are scaled by the corresponding values of an infinite granularity detector. The results indicate that the loss due to multiple hits affects the results significantly. The correction factors obtained for this depend both on multiplicity and the initial flow, and are due to the combined effect of the method and finite granularity. For an infinite granularity detector, the scaled values are 1, requiring no correction factors.

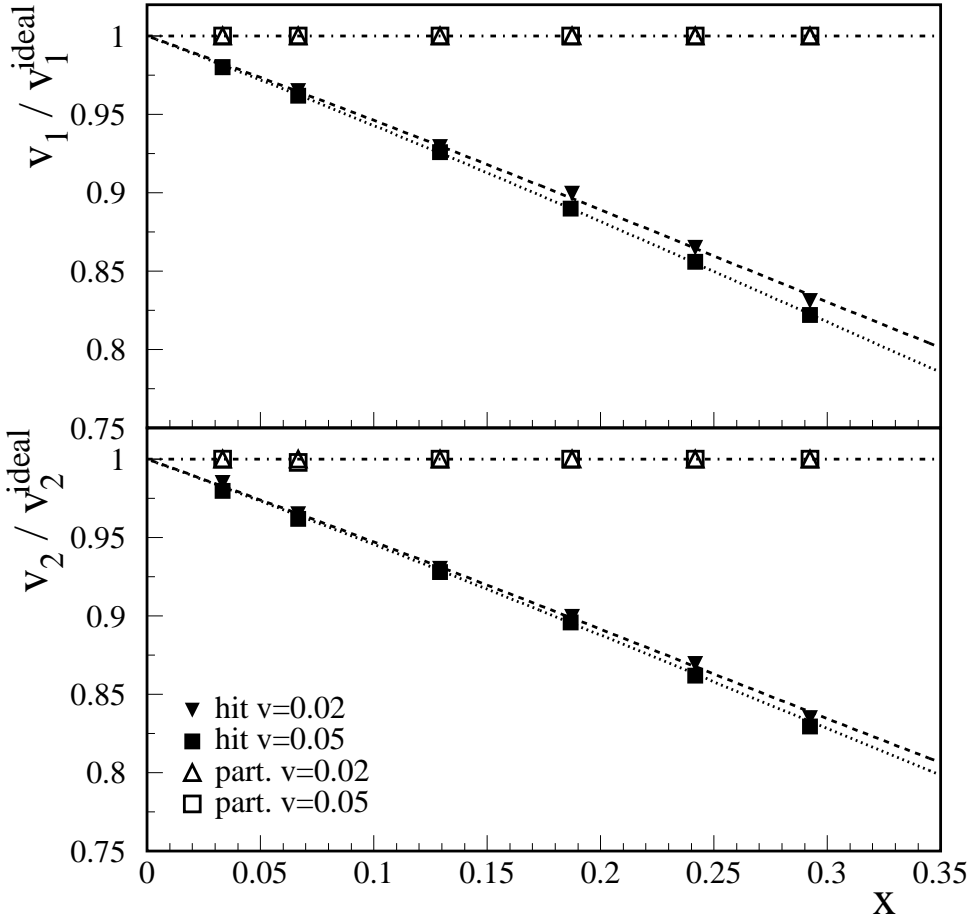


Figure 2: Open symbols show the ratio  $v_n^{ch}/v_n^{ideal}$  for different values of  $x$ . Filled symbols show the ratio  $v_n^{hits}/v_n^{ideal}$ . Squares are for  $v_n = 0.05$  and triangles are for  $v_n = 0.02$ . These results have been obtained using the known event plane angle in simulations. The top panel is for  $v_1$  and the bottom panel is for  $v_2$ . The dashed and dotted curves are equation 6 and equation 7 respectively. A horizontal line at the value of ratio equal to 1. is also drawn.

The dilution due to this method can be understood as follows: For an azimuthal distribution given by equation 8, the particle density is maximum along the direction of the reaction plane. On an event by event basis, the maximum loss of particles due to multiple hits will be along this direction. Consider there are  $N^{corr}$  correlated particles in a region  $\delta\phi$  about the reaction plane, where  $N^{corr}/N_{total}$  is greater than  $\delta\phi/2\pi$ . When such an event is divided into two equal multiplicity subevents, the correlation between the two sub events will be maximum if  $N^{corr}/2$  particles go into each subevent. Though this is true on the average, on an event by event basis, only a certain number out of  $N^{corr}$  fall into one subevent. The correlation between sub events for these events is less than the corresponding situation described above. The correlation will be weakest if all of these particles fall into one sub event. In such a situation, the  $v_n$  values are likely to be much lower than the  $v_n^{ideal}$ . However, the probability of the random sub division into this situation is  $(1/2)^{N^{corr}-1}$ , and is small.

The situation remains the same when hits are recorded instead of particles, and we replace  $N^{corr}$  by  $N_{hits}^{corr}$ , and  $N_{total}$  by  $N_{hits}$ . The probability of a random division with all  $N_{hits}$  going

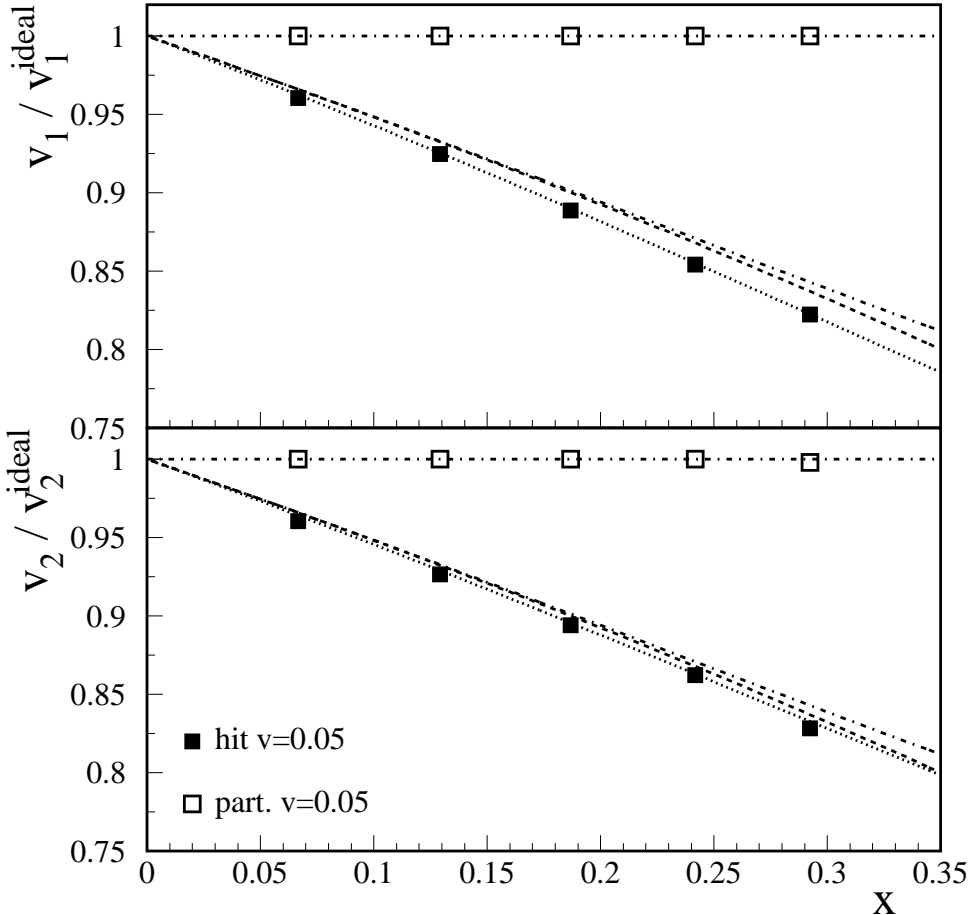


Figure 3: Open symbols show the ratio  $v_n^{ch}/v_n^{\text{ideal}}$  for different values of  $x$ . Filled symbols show the ratio  $v_n^{hits}/v_n^{\text{ideal}}$ . These results are for  $v_n = 0.05$  and are obtained from simulations. The dotted curve is equation 6 and the dashed curve is equation 7. The dash-dot curve corresponds to equation 6 without the term  $f(v)$ . A horizontal line at the value of ratio equal to 1. is also drawn.

into a sub event is  $(1/2)^{N_{\text{corr}}^{\text{hits}}-1}$ . This probability is clearly greater than the corresponding case where there is no loss of particles due to multiple hits. When this happens, the two subevents show little correlation, causing both  $v'_n$  and  $\text{RCF}_n$  to decrease. The decrease in both quantities only partially compensate each other and the resultant values are observed to be lower, as shown in the third panel of the figure, giving large values of correction factors. The resultant effect is to produce a reduced value of  $v_n$ , which would need a relatively larger correction factor to obtain the accurate value, as corroborated by simulations.

## 5 Conclusions

The finite granularity of the detector that measures the distribution of hits affects the details of the analysis methods that determine the anisotropy parameters. The uncertainty in the position of the angle due to finite azimuthal extent of the detector cell has a small effect. The major contribution arises due to loss of particle information due to multiple hits. The random division

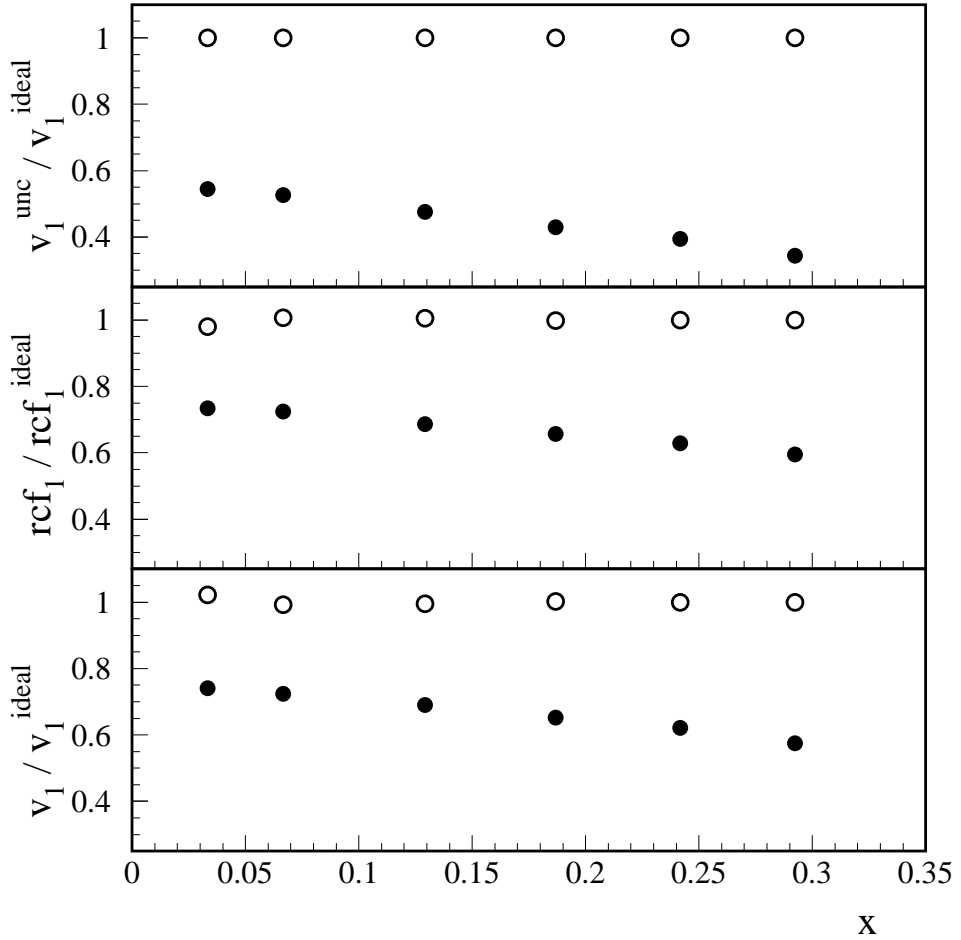


Figure 4: The results of method 4 described in the text are shown here. The panels from top show uncorrected values of  $v'_n$ , RCF and  $v_n$  for charged particles and hits for an initial flow 0.04. The values are scaled with corresponding values for the ideal case (infinite granularity detector). For the charged particles, the method is able to reproduce the initial flow, but the loss due to multihits causes very different contributions to  $v'_n$  and to RCF, giving much lower values of  $v_n$

into subevents dilutes the RCF and  $v'_n$  both, by unequal factors, affecting the resultant values of  $v_n$ . One must mention here that obtaining the Fourier coefficients for anisotropy determination is a two step process (i) obtaining the event plane and its resolution, RCF, the value of which is affected by the finite granularity of the detector used to measure particles that determine event plane. The poorer resolution of the event plane arising due to finite granularity is not corrected for by the event plane resolution as obtained in [2]. (ii)  $v'_n$  depends on the granularity of the detector measuring the set of particles used in its determination, and also on the granularity of the other detector used in event plane determination. The analysis and the discussion in the present work are suited for the case where the event plane is being determined from the same set of particles.

## References

[1] J.-Y. Ollitrault, Phys. Rev. **D46** (1992) 229.

- [2] A.M. Poskanzer and S.A. Voloshin, Phys. Rev. **C58** (1998) 1671
- [3] E877 Collaboration, J.Barette et.al., Phys. Rev. Lett. **73** (1994) 2532; Phys. Rev. Lett. **70** (1993) 2996; Phys. Rev. **C55** (1997) 1420; Phys. Rev. **C56** (1997) 3254.  
E802 Collaboration, L.Ahle et.al., Phys. Rev. **C57** (1998) 1416.
- [4] NA49 Collaboration, H. Appelshäuser et al., Phys. Rev. Lett. **80** (1998) 4136; C. Alt et al., Phys. Rev. **C68** (2003) 034903.
- [5] WA93 Collaboration, M.M. Aggarwal et.al., Phys. Lett. **B403** (1997) 390;  
Sudhir Raniwala, Pramana-Journal of Physics **60** (2003) 739;  
WA98 Collaboration, M.M. Aggarwal et.al., nucl-ex/**0406022**
- [6] CERES/NA45 Collaboration, J. Slivova et al., Nucl. Phys. **A715** (2003) 615c.
- [7] STAR Collaboration, K.H. Ackermann et al., Phys. Rev. Lett. **86** (2001) 402;  
C. Adler et al., Phys. Rev. Lett. **87** (2001) 182301.
- [8] PHENIX Collaboration, K. Adcox et al., Phys. Rev. Lett. **89** (2002) 212301. S. Esumi et al., Nucl. Phys. **A715** (2003) 599c.
- [9] PHOBOS Collaboration, B.B. Back et.al., Phys. Rev. Lett. **89** (2002) 222301. B. Back et al., nucl-ex/**0406021**
- [10] D. Molnar and S.A. Voloshin, Phys. Rev. Lett. **91** (2003) 092301
- [11] W.T. Lin et al., Nucl. Instrum. Meth. **A389** (1997) 415.
- [12] B. Alessandro et al., Nucl. Instrum. Meth. **A493** (2002) 30
- [13] Marek Idzik, private communication
- [14] J.-Y. Ollitrault, e-print nucl-ex/**9711003** (1997)